Applied Surface Science 255 (2009) 8084–8090

Contents lists available at ScienceDirect

Applied Surface Science

journal homepage: www.elsevier.com/locate/apsusc

Electrochemical and surface characterisation of carbon-film-coated piezoelectric quartz crystals

Edilson M. Pinto [a], Carla Gouveia-Caridade [a], David M. Soares [b], Christopher M.A. Brett [a,*]

[a] Departamento de Química, Faculdade de Ciências e Tecnologia, Universidade de Coimbra, 3004-535 Coimbra, Portugal
[b] Instituto de Física Gleb Wataghin, Unicamp, Campinas, SP, Brazil

ARTICLE INFO

Article history:
Received 26 March 2009
Received in revised form 8 May 2009
Accepted 8 May 2009
Available online 15 May 2009

Keywords:
Piezoelectric crystals
Electrochemical quartz crystal microbalance
Carbon
Electrochemistry
Atomic force microscopy

ABSTRACT

The electrochemical properties of carbon films, of thickness between 200 and 500 nm, sputter-coated on gold- and platinum-coated 6 MHz piezoelectric quartz crystal oscillators, as new electrode materials have been investigated. Comparative studies under the same experimental conditions were performed on bulk electrodes. Cyclic voltammetry was carried out in 0.1 M KCl electrolyte solution, and kinetic parameters of the model redox systems $Fe(CN)_6^{3-/4-}$ and $[Ru(NH_3)_6]^{3+/2+}$ as well as the electroactive area of the electrodes were obtained. Atomic force microscopy was used in order to examine the surface morphology of the films, and the properties of the carbon films and the electrode-solution interface were studied by electrochemical impedance spectroscopy. The results obtained demonstrate the feasibility of the preparation and development of nanometer thick carbon film modified quartz crystals. Such modified crystals should open up new opportunities for the investigation of electrode processes at carbon electrodes and for the application of electrochemical sensing associated with the EQCM.

1. Introduction

In recent years, the development and application of the quartz crystal microbalance, QCM, has grown in many fields of science. Many researchers are giving special attention to the development of materials such as diamond-like carbon films, polymeric films and nanostructured films [1–3]. Several research groups have developed in situ electrochemical quartz crystal mass sensors [4–7], and the electrochemical quartz crystal microbalance (EQCM) has been used to study the electrochemical dissolution of metal films [8–11].

Additionally, multisensor arrays on the same crystal have been recently proposed [12,13]. The QCM has also been used in thin film deposition monitors and in gas sorption and vapour sensors using carefully selected coating materials as the chemically active interface [14,15]. The high sensitivity of the quartz crystal microbalance is the basis for its application in thin film studies [16]. In the cases where the thin film coating serves simultaneously as an electrode the possibility of correlating the resonance frequency shift, Δf_q with the change of loading mass, Δm, given by Sauerbrey equation, is exploited for correlating charge transfer and mass transfer occurring at electrode-solution interfaces [17].

One of the main limitations of the EQCM is the fact that the piezoelectric quartz crystals have metallic thin film electrode coatings [18], which are restricted to a few metals, especially gold, and which are susceptible to form surface oxides or dissolve [19]. Such phenomena represent a limiting factor in electrochemical studies, particularly for the characterisation of processes which can occur at other electrode materials, and in the development of sensors and biosensors.

The principal requirements for a good electrode material are long-term stability, low residual current and wide potential range. As an alternative to metal electrodes in electrochemical sensors, carbon in various forms has emerged as a promising material with good physical and mechanical properties such as hardness and robustness, ease of surface regeneration, etc. [20–22]. Carbon-based materials as electrodes usually have a wider potential range than solid metal electrodes, can often pass higher currents and have long-term stability. The development and characterisation of new, carbon-based, non-toxic electrode materials for electrochemical sensors and biosensors has been an active field of research, [23], and which would benefit from complementary studies at carbon film EQCMs to better understand the adsorption, deposition and dissolution phenomena which take place at carbon electrode/electrolyte interfaces.

The objective of this work was to characterise the electrochemical properties of carbon films of thickness between 200 and 500 nm, sputter-coated on gold- and platinum-coated 6 MHz piezoelectric quartz crystal oscillators, and to evaluate the

* Corresponding author. Tel.: +351 239 835295; fax: +351 239 835295.
E-mail address: brett@ci.uc.pt (Christopher M.A. Brett).

0169-4332/$ – see front matter © 2009 Elsevier B.V. All rights reserved.
doi:10.1016/j.apsusc.2009.05.020

feasibility of using these films as electrode materials. Comparative studies were performed on bulk electrodes.

Cyclic voltammetry was used to examine the voltammetric characteristics, in particular to measure the potential window and to determine the electroactive area of the carbon-film-coated crystals. Atomic force microscopy (AFM) was used to evaluate the surface morphology of the films and electrochemical impedance spectroscopy was applied to investigate the properties of the carbon films and the electrode-solution interface.

2. Experimental

2.1. Reagents and electrolyte solutions

All solutions were prepared from analytical grade reagents and Millipore Milli-Q nanopure water (resistivity $\geq$18 MΩ cm) and the experiments were performed at room temperature, 25 $\pm$ 1 °C. The supporting electrolyte was 0.1 M potassium chloride, from KCl (Riedel-deHaën, Germany), containing 5 mM hexaammineruthenium(III) chloride (Riedel-de-Haën, Germany), or 5 mM potassium hexacyanoferrate(II) trihydrate (Fluka, Switzerland), as required.

2.2. Electrodes and preparation of carbon film coatings.

Electrodes were prepared from piezoelectric quartz crystals (KVG-Germany), 6 MHz with a geometric area of 0.28 cm^2 covered by Au and Pt. Thin carbon films of 500 nm thickness were deposited by rf magnetron sputtering (energy 1 keV) after washing the metal substrates in 0.1 M perchloric acid. The target material was produced by heating graphitic carbon.

A Pt foil, area 1.0 cm^2, was used as counter electrode and a saturated calomel electrode (SCE) (Radiometer, Denmark) was used as reference.

2.3. Instrumentation

Voltammetric studies were carried out with a microAutolab (EcoChemie, Netherlands), controlled by GPES Autolab software, connected to a home made QCM.

Electrochemical impedance spectra were recorded using a Solartron 1250 Frequency Response Analyser coupled to a Solartron 1286 Electrochemical Interface (Solartron Analytical, UK), controlled by ZPlot 3.0 software (Scribner Associates). A sinusoidal perturbation of 10 mV rms was applied over the frequency range 65.5 kHz–0.1 Hz, in 10 steps per decade, at applied potentials from −0.5 to +0.5 V vs. SCE, with 60 s auto-integration.

AFM images were recorded with a Multimode™ Atomic Force Microscope controlled by a Digital Instruments Nanoscope E controller (Veeco Instruments, USA). Silicon nitride NanoProbes™ V-shaped cantilevers, 100 μm length, 0.58 N m^{-1} spring constant were used. All images were recorded in contact mode AFM in air at room temperature.

3. Results and discussion

3.1. Cyclic voltammetry

3.1.1. Potential window

Cyclic voltammetry was used to investigate the potential window of carbon films sputter-deposited on Au and Pt quartz crystal electrodes in 0.1 M KCl solution, and comparison was made with Au and Pt electrodes to test whether the carbon film completely covers the metal substrate. No oxidation or reduction peaks should appear between the potential limits of hydrogen and oxygen evolution on the carbon-coated electrodes, unless they are due to chemical reactions of the film surface itself.

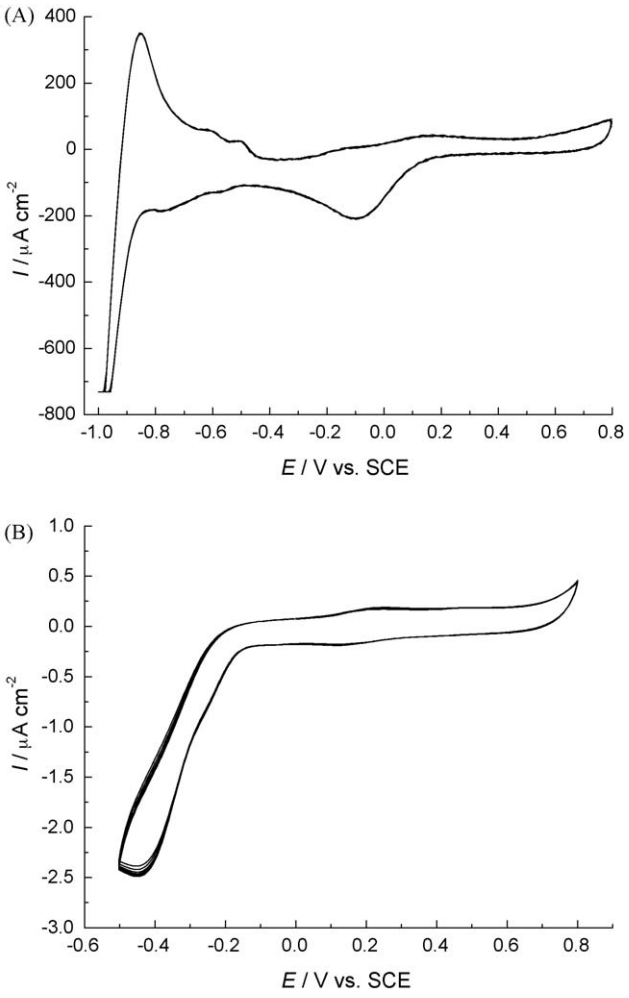

Fig. 1. Cyclic voltammograms (normalised to geometric area of the electrodes) obtained with (A) carbon-coated gold quartz crystal electrode, (B) gold quartz crystal electrode in 0.1 M KCl at 25 °C; 5 scans at 20 mV s^{-1}.

Fig. 1A and B shows cyclic voltammograms, normalized by the geometric area of the electrodes, obtained at carbon-film-coated gold quartz crystal (C/Au) and at bare gold quartz crystal (Au) electrodes, respectively, in 0.1 M KCl. In these cases, at potentials above +0.8 V vs. SCE there is a possibility to form a gold chloride complex $AuCl_4^-$ [24], which may afterwards be dissolved in the aqueous solution. The oxidation peak at +0.8 V at C/Au electrodes was ~90 μA cm^{-2}, which is much higher than that at Au electrodes (~0.4 μA cm^{-2}). At negative potentials, the hydrogen evolution potential shifted by around 0.4 V to more negative values with the C/Au electrode, starting at ~−0.9 V, compared with the Au electrode, where hydrogen evolution began to occur at ~−0.5 V; the peak at −0.2 V is due to reduction of surface oxides. This is a considerable increase in the negative potential limit into a region where Au electrodes cannot be used for electrochemical studies.

Cyclic voltammograms at carbon-film-coated Pt quartz crystal electrodes (C/Pt), recorded in 0.1 M KCl solution, are shown in Fig. 2. It is clearly observed that the negative limit of the potential window at the C/Pt electrode is much more negative (~−1.0 V vs. SCE) than at Pt electrodes, for which hydrogen evolution starts at around −0.2 V [25]. The positive potential limit was essentially the same at both electrodes. Background currents obtained with C/Pt electrodes are much lower than those obtained at C/Au electrodes. The higher background current at the C/Au electrode is related

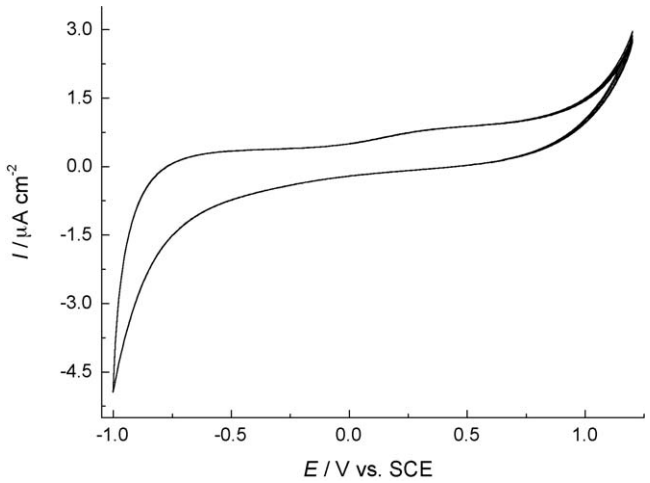

Fig. 2. Cyclic voltammograms (normalised to geometric area of the electrodes) obtained with carbon-coated Pt quartz crystal electrode in 0.1 M KCl at 25 °C; 5 scans at 20 mV s^{-1}.

with the oxidation/reduction of functional groups in the carbon film. This behaviour and magnitude of current are in agreement with other studies with pyrolytic carbon films [26]. The background current at C/Pt was lower, attributed to the formation of non-electroactive carbon structures when coating the Pt substrate with carbon film (see below also).

Thus, the two carbon modified electrodes, C/Au and C/Pt, show a wide potential window. The potential range of ~−0.9 V to +0.8 V for C/Au is less than that of C/Pt which has ~−1.0 V to +1.0 V. This widening of the negative potential range represents a great enhancement in the possible applications of electrodes used in EQCM studies.

3.1.2. Determination of electroactive area

Standard electroactive species were used to investigate the kinetic behaviour of model redox species and to determine the electroactive area of the new carbon modified quartz crystal electrodes.

Fig. 3A illustrates results obtained using cyclic voltammetry for reduction of 5 mM of hexaaminoruthenium(III) in 0.1 M KCl at C/Au electrodes; similar experiments were conducted for the reduction of 5 mM of hexacyanoferrate(III) in 0.1 M KCl electrolyte solution. The principal parameters obtained are summarised in Table 1. The expected characteristic peaks for reduction and oxidation of the electroactive species were observed in the voltammograms, with a slightly increased peak separation on increasing scan rate. Peak currents follow a linear relationship with the square root of the scan rate, as shown in the inset of Fig. 3A, and the ratio of peak currents is close to one, as predicted for the two redox systems under study.

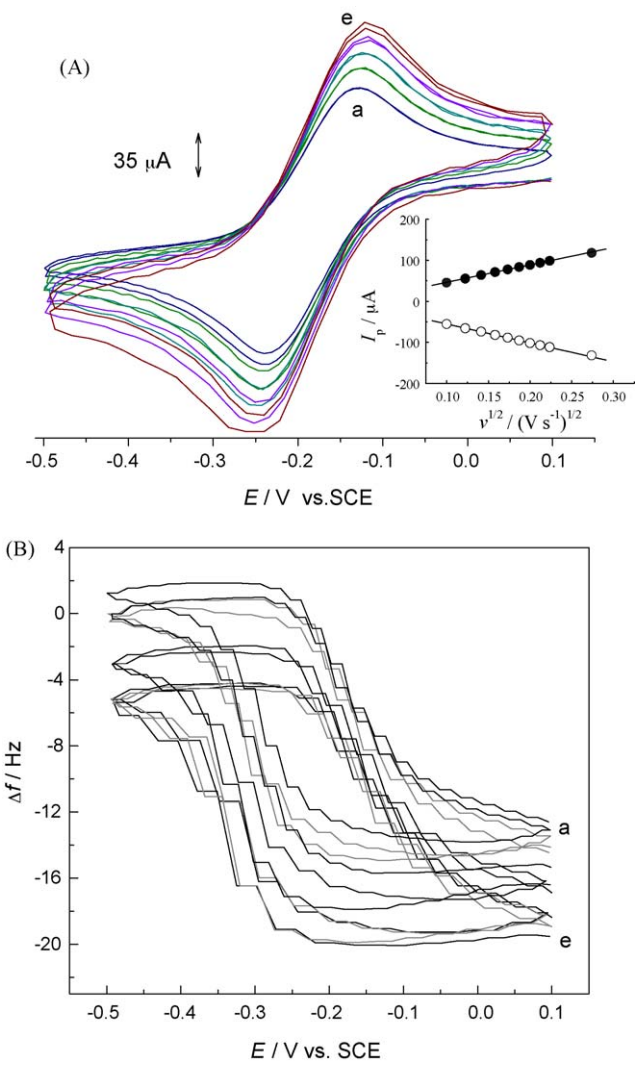

Fig. 3. (A) Cyclic voltammograms of 5 mM $Ru(NH_3)_6^{3+}$ in 0.1 M KCl at C/Au electrode (after base line subtraction) at scan rates from 0.01 to 0.05 V s^{-1} (a–e); and dependence of peak current on the square root of scan rate, (B) simultaneous frequency change, Δf, vs. potential recorded from 0.01 to 0.05 V s^{-1} (a–e).

The standard rate constant, k_0, was estimated according to Nicholson's method from the anodic and cathodic peak separation [27], giving values between (1.2 and 2.2) × 10^{-3} cm s^{-1}, which are lower than at the Au crystal (around 4.0 × 10^{-3} cm s^{-1} for the two redox systems), so that the kinetics is slower at C/Au than at Au. However, this commonly happens at carbon electrodes [20].

The electroactive areas of the electrodes were calculated from the reduction and oxidation peak currents obtained by cyclic

Table 1
Parameters obtained from the cyclic voltammograms of 5 mM $[Ru(NH_3)_6]^{3+}$ and $[Fe(CN)_6]^{3-}$ in 0.1 M KCl at C/Au electrode.

ν/V s^{-1}	$\lvert I_{pc}/I_{pa}\rvert$		ΔE_p/V		$k_0 \times 10^3$/cm s^{-1}	
	$[Ru(NH_3)_6]^{3+}$	$[Fe(CN)_6]^{3-}$	$[Ru(NH_3)_6]^{3+}$	$[Fe(CN)_6]^{3-}$	$[Ru(NH_3)_6]^{3+}$	$[Fe(CN)_6]^{3-}$
0.010	0.88	1.74	0.095	0.112	2.04	1.24
0.015	0.84	0.87	0.103	0.116	2.21	1.25
0.020	0.84	0.97	0.107	0.120	2.36	1.41
0.025	0.85	0.99	0.111	0.120	2.54	1.57
0.030	0.86	0.96	0.119	0.128	2.08	1.34
0.035	0.88	0.99	0.123	0.136	2.12	1.34
0.040	0.88	0.99	0.127	0.136	1.87	1.43
0.045	0.89	0.99	0.131	0.140	1.91	1.51
0.050	0.90	0.98	0.131	0.144	2.02	1.54
0.075	0.92	0.98	0.153	0.148	2.20	1.81

voltammetry, using the Randles–Sevick equation for reversible systems [25]:

$$I_p = 2.69 \times 10^5 n^{3/2} A D_O{}^{1/2} [O]_\infty \nu^{1/2} \quad (1)$$

where I_p is the peak current, A is the electroactive area, and D_O the diffusion coefficient of hexaaminеruthenium(III), 9.1×10^{-6} cm^2 s^{-1} [28], or hexacyanoferrate(III), 6.2×10^{-6} cm^2 s^{-1} [29].

From the slope of the lines in the inset of Fig. 3A for hexaaminеruthenium(III) reduction, the electroactive area of the C/Au electrode was calculated as ~0.16 cm^2; the same electroactive area was obtained for hexacyanoferrate(III) reduction. This electroactive area is ~57% of the geometric area of the electrode (0.28 cm^2) and ~84% of the calculated electroactive area of the Au electrode on the quartz crystal (~0.19 cm^2). The difference between C/Au and Au-coated crystals can be attributed to the fact that carbon sputtered on to the gold film can lead to many different forms of carbon, including conducting forms of carbon such as highly ordered pyrolytic graphite (HOPG) [21,30,31] as well as amorphous graphite and diamond-like carbon, which are not good conductors, leading to the lower electroactive area observed on the C/Au electrode.

Unfortunately, the C/Pt electrode led to poorly defined voltammograms, so that it was not possible to extract any information concerning the kinetics of the two standard redox couples, nor of the electroactive area. It suggests that Au substrates are superior for forming these types of sputtered carbon film.

The EQCM was used to study the reduction and oxidation of hexaaminеruthenium(III) by monitoring the mass change whilst recording the cyclic voltammograms, as shown in Fig. 3B, which presents the frequency variation, Δf_q, during two potential cycles at five different scan rates, from 0.01 to 0.05 V vs. SCE. All curves have a similar shape for all scan rates studied.

It is seen that the oscillation frequency values return to the initial values after two cycles for all five scan rates, reaching a maximum change of −14 Hz, indicating that no irreversible adsorption or desorption occurs on the electrode surfaces.

Contrary to the current response, which increases with scan rate, Fig. 3A, the maximum change in frequency during scanning decreases by ~2–3 Hz, Fig. 3B, which can be explained by the ionic concentration gradient close to the surface electrode increasing with the increase of scan rate.

3.2. AFM surface characterisation

Contact mode atomic force microscopy was used to examine the local morphological structures of unmodified Au and carbon film modified Au crystals in order to ascertain the differences between these two surfaces. Figs. 4 and 5 show 2D and 3D images of the Au and C/Au surfaces, respectively.

The images reveal that the Au crystal, Fig. 4, has a more regular and lower dimension of the nanostructures formed as well as a lower roughness and greater uniformity on the crystal surface, than does C/Au coated crystals, Fig. 5. It is clearly noticeable that the maximum height is higher on the C film from C/Au crystal, more than two times that of the height of the Au film surface.

The mean roughness, R_a, defined as the average absolute deviation of the roughness irregularities from the mean line over one sampling length [32] was found to be ~3.8 nm on the C film, which is more than three times that of the Au film, ~1.1 nm. These parameters were determined from an area of 9 μm^2, as shown in Figs. 4 and 5.

The structural differences obtained with the C/Au film are due to the formation of various different forms of carbon by sputtering, as discussed above.

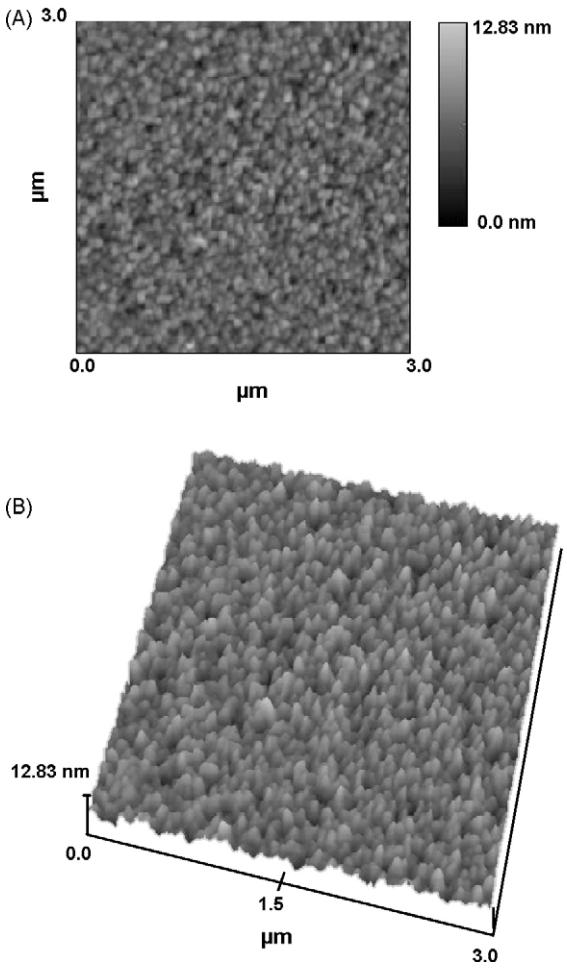

Fig. 4. AFM topographical images of Au crystal in (A) 2D and (B) 3D.

In recent work [26] carried out with carbon film electrodes made from carbon film resistors of various nominal resistances, produced from the pyrolysis of methane, the same behaviour was found. It was revealed that the carbon films on the ceramic substrates can include different types of carbon, the graphitic structure being larger in proportion than the other types of carbon. On electrodes of higher nominal resistance greater roughness in the AFM images and less well-defined electrochemical profiles were obtained, which were related with the structural composition of the film. In the films studied here, there was probably a larger amount of amorphous carbon and other types of non-conductive carbon, leading to lower electroactivity.

Long-term stability of these carbon-coated crystals has been observed - there is evidence of good adherence of the carbon films, in these morphological and also in the electrochemical studies, which results from the high sputtering energy applied, 1 keV, permitting "injection" of carbon atoms into the gold (or platinum) film, and carbon atom intercalation with gold (or platinum) atoms on the surfaces. The roughness of the metal substrate film also plays an important role since the carbon atoms can fill the cavities creating stronger adherence.

3.3. Electrochemical impedance spectroscopy

The interfacial characteristics of the Au and carbon-coated metal electrodes were studied by EIS. Experiments were carried out at applied potentials from +0.5 to 0.0 V vs. SCE, chosen after analysing the cyclic voltammograms (see Fig. 1). This potential

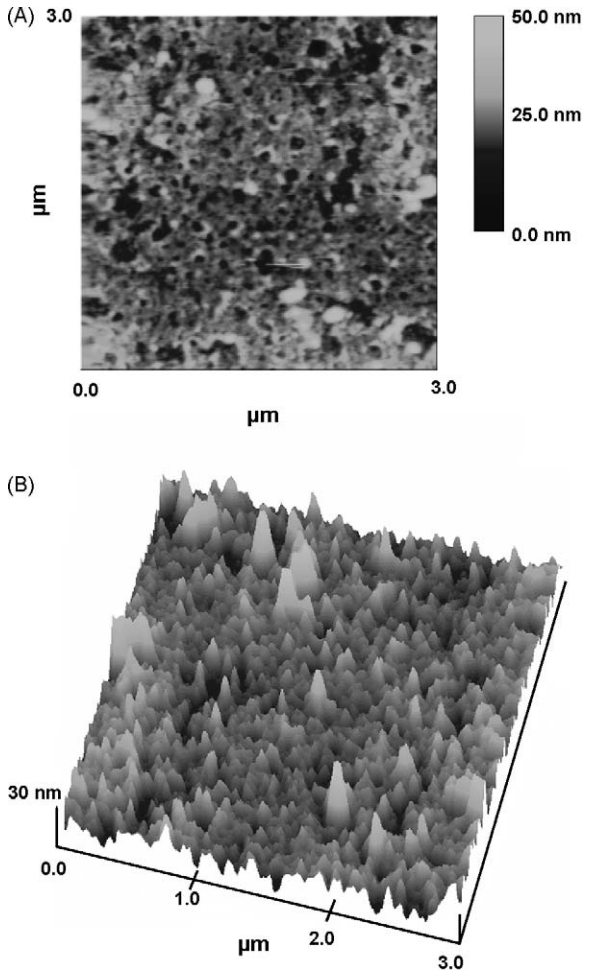

Fig. 5. AFM topographical images of C/Au crystal in (A) 2D and (B) 3D.

range allows a detailed comparison between C/Au and Au electrodes and comparison with C/Pt. Spectra recorded at +0.50, +0.25 and 0.0 V vs. SCE are shown in Fig. 6.

Modified Randles circuits were used to model the spectra at all electrodes, Fig. 7A and B, in which the CPE_f represents the capacitance of the film and R_f its resistance. The other part of the circuits represents the charge transfer resistance, R_{ct}, and the double layer capacitance, C_{dl}, or CPE_{dl} in the case of Au electrodes. The constant phase element $CPE = \{(C\,i\omega)^n\}^{-1}$ models a non-ideal capacitor in all cases and was found to be necessary due to the non-homogeneity of the surfaces; values of n between 0.5 (porous electrode) and 1 (smooth electrode) are possible. The equivalent circuit used, in Fig 7B, to model the C/Au and C/Pt electrodes is used mostly in cases of organic coatings on metal surfaces [33,34], chosen here since the carbon-coated electrodes can be expected to have similar electrical characteristics to the organic coatings, also deposited on metal substrates. It is also considered that they have a low porosity, justifying the need for ($R_{ct}C_{dl}$).

Table 2 summarises circuit component values obtained by fitting the spectra at all potentials studied. The n exponent has a typical value of ~0.80 for C/Au, C/Pt and Au electrodes. Values of cell resistance, R_Ω, were ~49 and ~47 Ω cm^2 for C/Au and Au electrodes and ~72 Ω cm^2 for C/Pt.

The OCP were 0.19, 0.15 and 0.11 V vs. SCE for C/Au, C/Pt and Au electrodes, respectively. Table 2 shows that between the limits of the potentials defined by the OCP for all electrode assemblies, *i.e.*, between +0.10 V and +0.20 V, the capacitance and resistance values do not change significantly for each electrode.

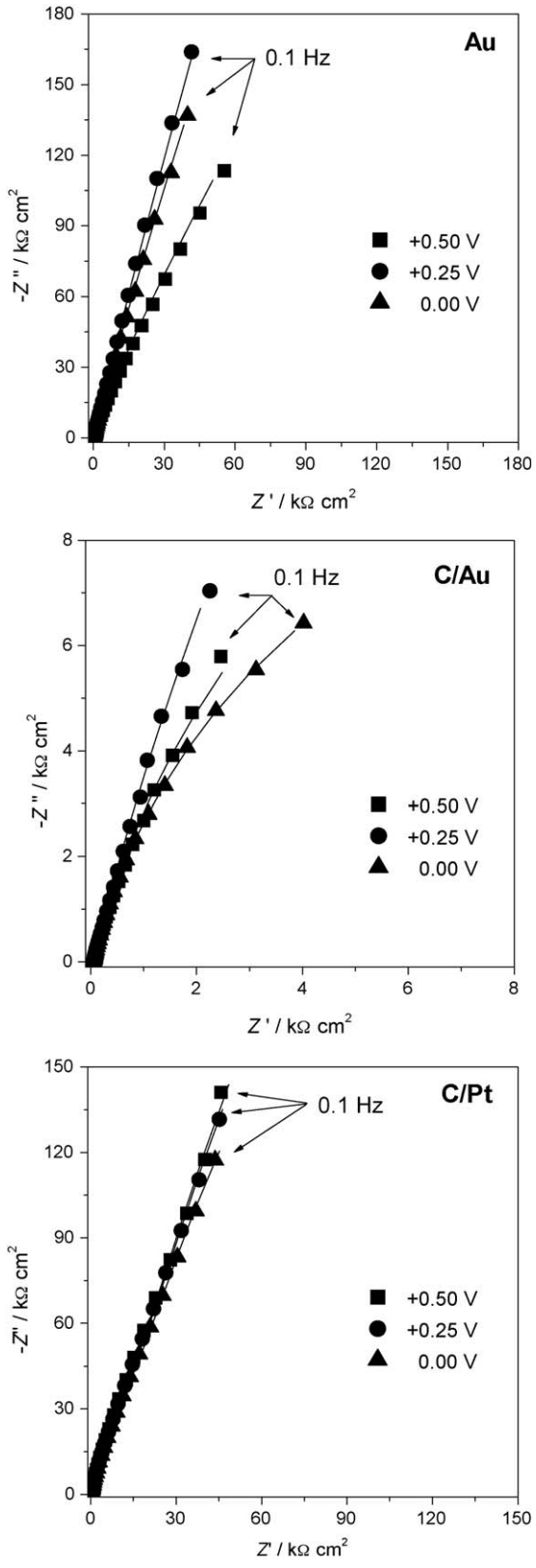

Fig. 6. Complex plane impedance plots in 0.1 M KCl of: (A) Au, (B) C/Au and (C) C/Pt electrodes at (▲) 0.00 (●) +0.25 and (■) +0.50 V vs. SCE. Lines represent the fitting to equivalent electrical circuits in Fig. 7.

Table 2
Equivalent circuit modelling of the impedance spectra in Fig. 6, using the equivalent circuits shown in Fig. 7A (Au) and 7B (C/Au, and C/Pt).

E/V vs. SCE	C_f/μF cm^{-2} s^{n-1}			R_f/kΩ cm^2		C_d/μF cm^{-2} (CPE_{dl}/μF cm^{-2} s^{n-1} for Au)			R_{ct}/kΩ cm^2		
	Au	C/Au	C/Pt	C/Au	C/Pt	Au	C/Au	C/Pt	Au	C/Au	C/Pt
0.50	5.03	206	7.55	0.03	241	6.74	2.19	3.06	2.32	34.9	1090
0.40	4.93	214	7.61	0.16	240	3.61	1.02	3.13	4.01	75.6	1040
0.30	5.41	196	7.75	0.03	232	3.10	2.24	2.14	5.64	12.2	1070
0.20	5.55	176	8.97	0.04	196	3.63	1.70	4.01	3.83	16.0	728
0.10	5.81	174	8.29	0.03	215	4.03	1.70	3.43	3.08	16.4	893
0.00	6.34	158	8.81	0.04	215	4.10	1.47	3.91	3.23	23.0	732

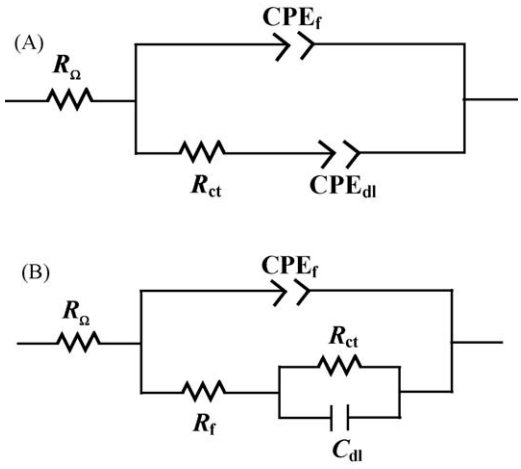

Fig. 7. Equivalent circuits used to fit the impedance spectra (A) Au electrodes and (B) C/Au and C/Pt.

It is seen from the spectra in Fig. 6, that the carbon coatings decrease the impedance values. As seen from the values in Table 2, for the unmodified Au electrode, Fig. 6A, the film capacitance, expressed by C_f, reaches a maximum value of 6.34 μF cm^{-2} s^{n-1} at 0.0 V and a minimum of 4.93 μF cm^{-2} s^{n-1} at +0.40 V. However, the charge transfer resistance, $R_{ct,}$ increases from 2.32 kΩ cm^2 at +0.50 V to 5.64 kΩ cm^2 at +0.30 V, and decreases again at 0.00 V to 3.23 kΩ cm^2. This increase and the subsequent decrease as the potential becomes more negative may be due to changes in the ease of charge transfer.

For the modified C/Au electrode, Fig. 6B, the film capacitance, C_f, reaches values of almost 40 times higher then those of the pure Au electrode, with a maximum of 214 μF cm^{-2} s^{n-1} at +0.40 V and a minimum of 158 μF cm^{-2} s^{n-1} at 0.00 V. The dependence of the double layer capacitance with the applied potential has the same behaviour as for the Au electrode. However, the carbon film coating has a double layer capacitance approximately three times smaller than that of bare Au electrodes, and the corresponding R_{ct} was higher, with a maximum value of 75.6 kΩ cm^2 at +0.40 V and a minimum of 12.2 kΩ cm^2 at +0.30 V.

The carbon-coated platinum electrodes, C/Pt, were studied in order to clarify the influence of the metal substrate sputtered on the quartz crystals on the electrochemical properties of the carbon film coating. Complex plane spectra for C/Pt are shown in Fig. 6C. It was observed that the C/Pt electrode presents higher capacitance values, especially at +0.50 and 0.00 V vs. SCE. Higher charge transfer resistances were observed at C/Pt compared to C/Au, a maximum of almost 30 times higher at +0.50 V, and the film resistance, R_f, at C/Pt was very high, with a maximum value of 241 kΩ cm^2 at +0.50 V. Thus, there is an influence of the underlying metallic substrate, with C/Au presenting better electrochemical properties than C/Pt.

Differences in surface area can contribute to the differences in capacitance and resistance values of carbon-coated and uncoated electrodes, since the quantitative values of these physical quantities depend on the electrode area. AFM morphological studies suggest that both types of carbon-coated electrodes have higher surface areas than pure metal electrodes, see Figs. 3 and 4, although not all of this is electrochemically active, as discussed above.

Summarising, the results show that carbon coating of Pt electrodes leads to a significant decrease of the electrical conductivity probably due to the formation of non-conducting carbon species during deposition, which bind to the metal surface. The decrease of the C/Au electrical conductivity, which occurs to a lesser extent, can be attributed to difficulties in electron transfer through the energy barriers at the gold–carbon and carbon-electrolyte interfaces.

C/Au appears to be preferable for future electrochemical and EQCM studies than the C/Pt electrode. It has already been used successfully, as demonstrated here, and future studies will address how to achieve a good surface activity whilst reducing the background currents. Besides providing a carbon surface, it also has a wider potential window than Au electrodes and does not suffer from the problems caused by the oxidation of gold at around +0.8 V vs. SCE.

4. Conclusions

Carbon film modified Au- and Pt-coated quartz crystals, C/Au and C/Pt, have been prepared and characterised electrochemically. Voltammetric studies show that C/Au and C/Pt have a wider potential window than without carbon. Calculation of the electroactive area using model redox couples shows that it is ~18% smaller for carbon-coated Au electrodes compared with bare Au electrodes, and with slower kinetics. Unfortunately, the C/Pt electrode showed poorly defined voltammograms, and it was not possible to extract any kinetic information or estimate the electroactive area.

Electrochemical impedance spectroscopy also shows that the C/Au electrodes present better electrochemical behaviour than C/Pt electrodes, which become more resistive after carbon deposition. This can be attributed to the formation of different carbon/platinum species during film deposition which can cover the electrode surface.

The results obtained demonstrate the feasibility of the preparation and development of nanoscale thickness carbon film modified quartz crystals, with good long-term stability. Carbon/gold crystals should open up new opportunities for the investigation of electrode processes at carbon electrodes and for the application of electrochemical sensing associated with the EQCM.

Acknowledgment

Financial support from Fundação para a Ciência e a Tecnologia (FCT), PTDC/QUI/65255/2006 and PTDC/QUI/65732/2006, POCI 2010 (co-financed by the European Community Fund FEDER) and CEMUC® (Research Unit 285), Portugal, is gratefully acknowledged.

CGC and EMP thank FCT for a postdoctoral fellowship (SFRH/BPD/46635/2008) and PhD grant (SFRH/BD/31483/2006), respectively. The authors are very grateful for technical support given by Luiz Bonugli and Carlos Lambert, IFGW, Unicamp, Brazil.

References

[1] J. Moon, S. Park, Y. Lee, G.S. Bang, J. Electroanal. Chem. 464 (1999) 230.
[2] H.J. Zeng, Y. Jiang, G.Z. Xie, J.S. Yu, Sens. Actuator B Chem. 122 (2007) 1.
[3] T.W. Chao, C.J. Liu, A.H. Hsieh, H.M. Chang, Y.S. Huang, D.S. Tsai, Sens. Actuator B Chem. 122 (2007) 95.
[4] T. Nomura, M. Ijima, Anal. Chim. Acta 97 (1981) 131.
[5] S. Bruckenstein, M. Shay, Electrochim. Acta 30 (1985) 1295.
[6] M. Benje, M. Eiermann, U. Pitterman, K.G. Weil, Ber. Bunsen-Ges, Phys. Chem. Chem. Phys. 90 (1986) 435.
[7] S. Bourkane, C. Gabrielli, M. Keddam, Electrochim. Acta 34 (1989) 1081.
[8] E. Müller, Praktikum der Electrochemie, Stein-Kopp Verlag (1953).
[9] S. Bruckenstein, S. Swathirajan, Electrochim. Acta 30 (1985) 851.
[10] H.J. Schmidt, U. Pittermann, H. Schneider, K.G. Weil, Anal. Chim. Acta 273 (1993) 561.
[11] A. Jardy, A.L. Lasalle-Molin, M. Keddam, H. Takenouti, Electrochim. Acta 37 (1992) 2195.
[12] T. Abe, M. Esashi, Sens. Actuator A Phys. 82 (2000) 139.
[13] P. Boecker, G. Horner, S. Rösler, Sens. Actuator B Chem. 70 (2000) 37.
[14] W.H. King, Anal. Chem. 36 (1964) 1735.
[15] C.K. O'Sullivan, G.G. Guilbault, Biosens. Bioelectron. 14 (1999) 663.
[16] M.D. Ward, D.A. Buttry, Science 249 (1990) 1000.
[17] G. Sauerbrey, Z. Phys. 155 (1959) 206.
[18] A.A. Vives (Ed.), Piezoelectric Transducers and Applications, second ed., Springer, Berlin, 2008.
[19] K. Watling, G.A. Hope, R. Woods, J. Electrochem. Soc. 152 (2005) D103.
[20] B. Uslu, S.A. Ozkan, Anal. Lett. 40 (2007) 817.
[21] N.Y. Stozhko, N.A. Malakhova, M.V. Fyodorov, K.Z. Brainina, J. Solid State Electrochem. 12 (2008) 1185.
[22] N.Y. Stozhko, N.A. Malakhova, M.V. Fyodorov, K.Z. Brainina, J. Solid State Electrochem. 12 (2008) 1219.
[23] C. Gouveia-Caridade, C.M.A. Brett, Electroanalysis 17 (2005) 549.
[24] J.C. Hoogvliet, W.P. van Bennekom, Electrochim. Acta 47 (2001) 599.
[25] C.M.A. Brett, A.M. Oliveira-Brett, Electrochemistry: Principles, Methods and Applications, Oxford University Press, Oxford, 1993.
[26] C. Gouveia-Caridade, D.M. Soares, H.-D. Liess, C.M.A. Brett, Appl. Surf. Sci. 254 (2008) 6380.
[27] R.S. Nicholson, Anal. Chem. 37 (1965) 1351.
[28] F. Marken, J.C. Eklund, R.G. Compton, J. Electroanal. Chem. 395 (1995) 335.
[29] H. Maleki, C.D. Cojocaru, C.M.A. Brett, G.M. Jenkins, J.R. Selman, J. Electrochem. Soc. 145 (1998) 721.
[30] P.K. Chu, L. Li, Mater. Chem. Phys. 96 (2006) 253.
[31] A. Zeng, E. Liu, S. Zang, S.N. Tan, P. Hing, I.F. Annergren, J. Gao, Thin Solid Films 426 (2003) 258.
[32] E.S. Gadelmawla, M.M. Koura, T.M.A. Maksoud, I.M. Elewa, H.H. Soliman, J. Mater. Process Technol. 123 (2002) 133.
[33] P. Bonora, F. Deflorian, L. Fedrizzi, Electrochim. Acta 41 (1996) 1073.
[34] J.M. Mcintyre, H.Q. Phan, Prog. Org. Coat. 27 (1996) 201.